[P8]

J. Villanen, P. Suvikunnas, C. Icheln, J. Ollikainen, and P. Vainikainen, “Performance analysis and design aspects of mobile terminal multi-antenna configurations,” *IEEE Transaction on Vehicular Technology*, to appear in march 2008 issue.

Performance Analysis and Design Aspects of Mobile Terminal Multi-Antenna Configurations

Juha Villanen, Pasi Suvikunnas, Clemens Icheln, Jani Ollikainen, *Member, IEEE*, and Pertti Vainikainen, *Member, IEEE*

***Abstract*— This paper presents a comprehensive study on the performance analysis and design aspects of mobile terminal multi-antenna configurations. Four realistic multi-antenna terminals are studied in a large set of measured SIMO and MIMO environments. Several performance metrics, such as the total efficiencies of the antenna configurations, envelope correlation, Effective Array Gain (*EAG*), eigenvalue dispersion, and capacity are used in the performance evaluation. Emphasis has been put on increasing understanding on the power transferring properties of mobile terminal multi-antenna configurations, for which purpose the *EAG* is used. Also, efficient theoretical ways of predicting the empirical *EAG* results based on the simulated 3-D radiation patterns of an antenna configuration are proposed and studied. The results of this paper provide novel and useful information for the designers of future multi-antenna terminals.**

***Index Terms*— Envelope correlation, Effective Array Gain, Multi-antenna, Capacity, Eigenvalue dispersion**

I. Introduction

The so-called SIMO (Single-Input Multiple-Output) systems with single transmit antenna and multiple receive antennas offer a well-known way to mitigate fast fading in wireless communications systems [1]-[3]. In recent years, many realistic internal diversity antenna configurations have been proposed for modern mobile terminals, e.g. [4]-[11]. Emphasis in diversity analysis has been in the evaluation and prediction of diversity gain [1], or the so-called effective diversity gain [12],[13]. The problem with diversity gain-based performance measures is that the antenna configuration's ability to capture energy from incident plane waves is not reliably characterized under realistic channel conditions, as demonstrated in [14]. With effective diversity gain this problem is not present if angular distribution of incident waves is uniform over the sphere, as assumed in [10]-[13]. In practice, however, the angular distribution is not uniform [15]. In diversity analysis, often also the Mean Effective Gains (*MEG*) [16],[17] of single antenna elements have been estimated [4]-[7],[9]-[11]. Total effective gains of the antenna configurations, however, have not been analyzed, predicted, and related to other performance metrics.

Transmission systems with multiple antennas at both ends of a radio link, i.e. MIMO (Multiple-Input Multiple-Output) systems, offer potential for large spectral efficiencies [18]-[20]. In recent years, numerous studies on the effect of receiving antenna on MIMO system performance have been published, e.g. [21]-[28]. In only a few of these studies [21]-[24], however, realistic models have been used for the combination of the metallic chassis of a mobile terminal and the internal antenna elements. Realistic modeling of the chassis in the analysis of a MIMO system is extremely important, as the wavemodes of the chassis can have significant contribution on the total power radiated by the terminal [29], and thus on the polarizations, directivities and shapes of the radiation patterns. In [21]-[24], the effects of such indicators and parameters on MIMO capacity (or Bit Error Rate [24]) were studied as correlation properties of a channel matrix [21],[23],[24], orientation of a mobile terminal [24], mutual coupling between transmit or receive antennas [22], *MEG*s of single antenna elements [23], and radiation efficiency of an antenna configuration [21]. Obviously, an antenna performance indicator capturing the effects of all these parameters would be a useful tool for an antenna designer. Such an indicator, named as Effective Array Gain (*EAG*), has been introduced in [25].

The paper at hand is continuation for [14]. In this paper, four realistic mobile terminal multi-antenna configurations are evaluated in 12 measured environments with a tool named measurement-based antenna test bed (MEBAT) [30]. All four antenna configurations are studied in free space, and two of them are further evaluated in the talk-position beside human head and hand models, resulting in total 72 antenna configuration-environment-combinations. Emphasis in the work has been put on the prediction and understanding of the power transferring properties of multi-antenna configurations in SIMO and MIMO systems. For that purpose, the idea of the *EAG* is used, and its connection to other important performance metrics and antenna parameters, such as total efficiency and radiation pattern properties of a multi-antenna configuration, envelope correlation, and the capacity of a

Manuscript first received June 13, 2006. This work was supported in part by the Graduate School of Electrical and Communications Engineering, Emil Aaltonen Foundation, HPY Foundation, and Nokia Foundation.

J. Villanen was with the Helsinki University of Technology, SMARAD, Radio Laboratory. He is now with the Nokia Corporation, FI-90571 Oulu, Finland (e-mail: juha.villanen@nokia.com).

P. Suvikunnas, C. Icheln, and P. Vainikainen are with the Helsinki University of Technology, SMARAD, Radio Laboratory, FI-02150 Espoo, Finland (e-mail: pertti.vainikainen@tkk.fi).

J. Ollikainen is with the Nokia Research Center, FI-00045 Helsinki, Finland.

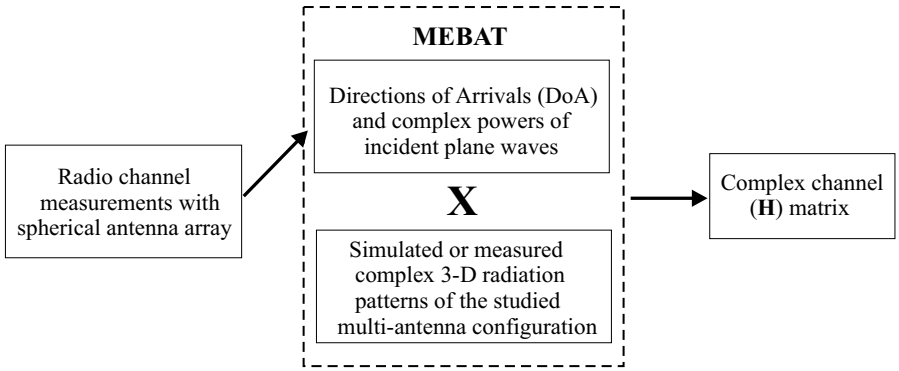

Fig. 1. A block-diagram of the basic working principle of MEBAT.

MIMO system are studied. In the MIMO analysis, also the so-called eigenvalue spread [31] is used as a performance metric. In addition to the above, a fast and accurate theoretical way of predicting the empirical *EAG*s is proposed. According to the author's knowledge, as extensive experimental studies as this work, conducted with realistic phone models and measured environments, have not been reported before.

The paper has been organized as follows. First, the operating principle of MEBAT is shortly introduced. After this, the studied multi-antenna configurations and their most important properties are presented. In the following chapter, the environments used in the study are introduced. This is followed by presentation of the applied computation and analysis methods. Finally, the results obtained with MEBAT are discussed and analyzed, and conclusions are given.

II. Measurement-Based Antenna test Bed (MEBAT)

A block-diagram of the basic working principle of MEBAT is presented in Fig. 1. A detailed description of MEBAT together with a thorough study on its accuracy is presented in [30]. As shown in Fig. 1, MEBAT relies on radio channel measurements made beforehand. The radio channels used in this study were selected from the channel library of the Radio Laboratory of the Helsinki University of Technology (TKK).

The selected channels have been earlier measured at 2.154 GHz with a wide-band radio channel sounder and a spherical dual-polarized antenna array. In the radio channel measurements, the spherical antenna array and the channel sounder have been located on a motorized trolley, which has been moved along a certain measurement route at the desired speed. The arrival angles and powers of the incident signals as a function of the location of the spherical antenna array have been estimated from measured channel impulse responses using beam-forming. The method enables the separation of signal multipath components with the same excess delay and Doppler shift as long as their angular separation is not less than 40º, and path loss difference more than 12 dB. The cross polarization discrimination is 17 dB, and the *rms* error of the incidence angle measurement is approximately 1º. The system can thus well describe the signal environment of a small mobile terminal antenna [33]. Detailed descriptions of the radio channel measurement system, data post-processing, and error sources of the measurement system can be found from [32],[33].

In MEBAT, the directions-of-arrival and power estimates of the incident multipath components are convolved with the complex 3-D radiation patterns of the antenna configuration under study (AUT). Either simulated or measured radiation patterns can be used. As an outcome, the complex channel matrix (**H**-matrix) of the whole system as a function of the location of the antenna configuration, including the effects of the transmitting and receiving antennas, is obtained. One of the main advantages of MEBAT is that the antenna configurations under study can be accurately evaluated in real propagation environments already during the early simulation phase of the antenna design process. Moreover, the radio channel stays exactly the same for all studied antenna configurations.

III. Studied Multi-Antenna Configurations

A. Antenna Geometries

During the work, four mobile terminal multi-antenna configurations (A1 – A4) for UTMS system were designed and evaluated. The coordinate system and the geometries of A1, A2, A3 and A4 are presented in Fig. 2. Antenna configurations A1 – A3 consist of two square-shaped single-band PIFAs (Planar Inverted-F Antenna) of size 16 x 16 x 7 mm^3 (width x length x height) placed on top of ground planes of size 40 x 100 x 3 mm^3 (width x length x thickness). In A3, the short circuit and the feed probe are placed such that the radiating open ends of the patches are located as far a way from each other as possible to increase isolation between the patches. In A2, the open ends are purposefully placed next to each other to decrease the isolation between the patches. Antenna configuration A4 comprises of a multi-band PIFA placed on top of the upper end of a ground plane, and an IFA (Inverted-F Antenna) placed at the same end of the ground plane. Detailed description of the multi-band PIFA, together with its simulated and measured performance is found from [34].

B. Simulation Methods

All four antenna configurations were simulated in free space with IE3D. In IE3D simulations, the antenna configurations were aligned on standard spherical coordinate system

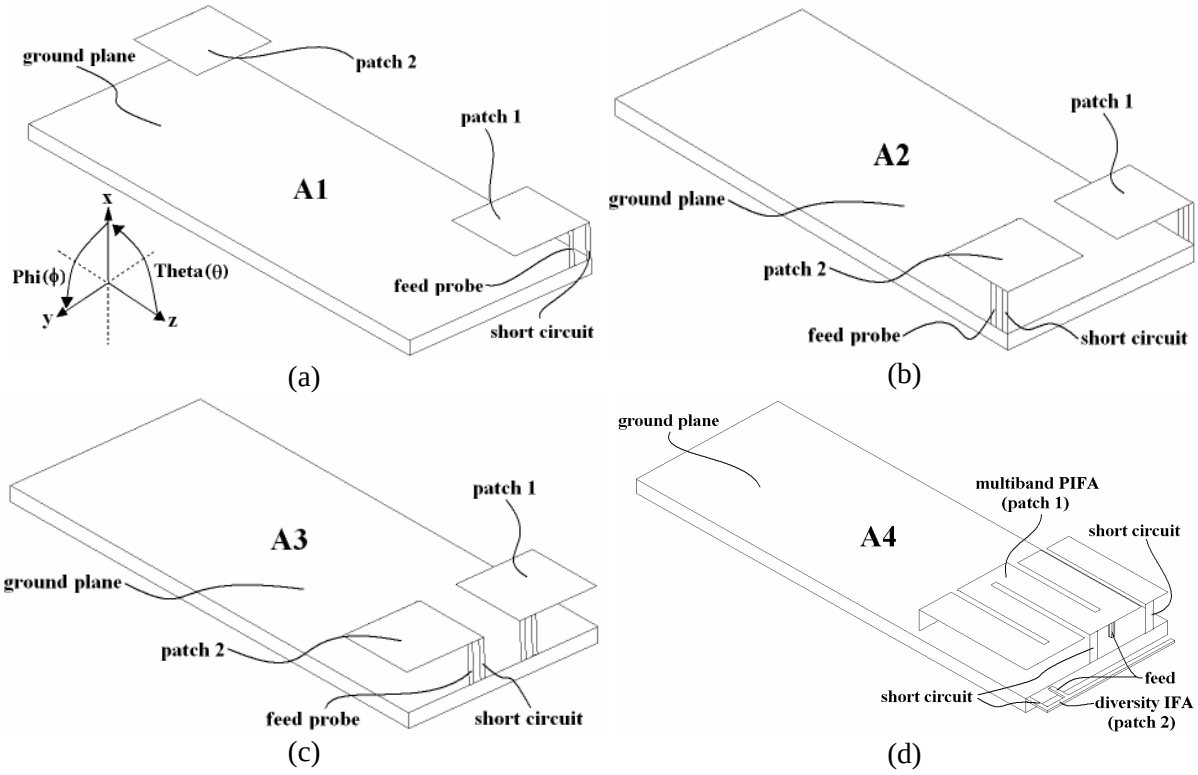

Fig. 2. Geometries of antenna configurations (a) A1 (b) A2 (c) A3 and (d) A4, and the coordinate system used in free space.

according to Fig. 2. Antenna configurations A3 and A4 were further simulated with XFDTD in talk position beside human head and hand models (later denoted by "HH"). The antenna configurations were located on the right side of a homogenous head model in the standard talk position, with the nose of the head model pointing towards the positive x-axis. The distance between the backside surface of the chassis and the ear of the head phantom was 7.0 mm in all simulations. The hand of the user was modeled with the hand model 2 published in [35].

C. Isolations, S-Parameters and Efficiencies

Table I presents the simulated radiation and total efficiencies, isolations (S_{21}) between the diversity elements, and reflection coefficients (S_{11}) obtained at 2.154 GHz. The total efficiencies can be obtained from the radiation efficiencies by taking into account impedance matching losses. The isolations of A1, A3 and A4 are relatively high in free space, larger than 12 dB. Owing to the relatively closely spaced open ends of the antenna elements of A2, the isolation of A2 is lower, only 5.4 dB. For this reason, also its radiation and total efficiencies in free space are somewhat lower than those of the other antenna configurations. In talk-position, the radiation efficiencies of A3 and A4 are clearly lower than in free space, as expected. Especially the efficiency of patch 2 of A4, i.e. the diversity IFA, suffers from the presence of the head and hand models. All four antenna configurations cover the UMTS band with impedance matching criterion $S_{11} \leq -6$ dB. The multiband PIFA of A4 additionally covers the operating bands of the E-GSM900, GSM1800, and GSM1900 systems [34].

D. Radiation Patterns

As the angular power spectrum in real propagation environments is usually not uniform, the shapes, orientations and polarizations of radiation pattern main lobes play an important role in defining mobile communications system performance. Fig. 3 presents simulated (at 2.154 GHz) 3-D realized gain patterns of the studied antenna configurations. Also polarization ellipses [36] are shown. The reported gain values include the effect of impedance matching losses. A narrow vertically oriented ellipse can be interpreted as vertical polarization. The same logic applies for horizontal polarization. In the used coordinate system, elevation angle theta = 90° represents the azimuth plane. The most important properties of the radiation patterns and their influence on multi-antenna performance are discussed later in this paper.

TABLE I, SIMULATED ISOLATIONS, REFLECTION COEFFICIENTS (S11), TOTAL EFFICIENCIES, AND RADIATION EFFICIENCIES (P1=PATCH 1 AND P2=PATCH 2).

	A1	**A2**	**A3**	**A4**	**A3HH**	**A4HH**
Isolation [dB]:	13.4	5.4	14.0	12.2	8.5	12.9
S_{11} (p1/p2) [dB]:	-8.1/-8.1	-12.0/-12.0	-6.7/-6.7	-8.8/-7.3	-10.2/-10.5	-11.6/-8.5
Total efficiency (p1/p2) [dB]:	-1.0/-1.0	-2.0/-2.0	-1.4/-1.4	-1.1/-1.3	-4.4/-5.1	-3.7/-6.8
Radiation efficiency (p1/p2) [dB]:	-0.3/-0.3	-1.6/-1.6	-0.3/-0.3	-0.5/-0.4	-4.0/-4.7	-3.4/-6.1

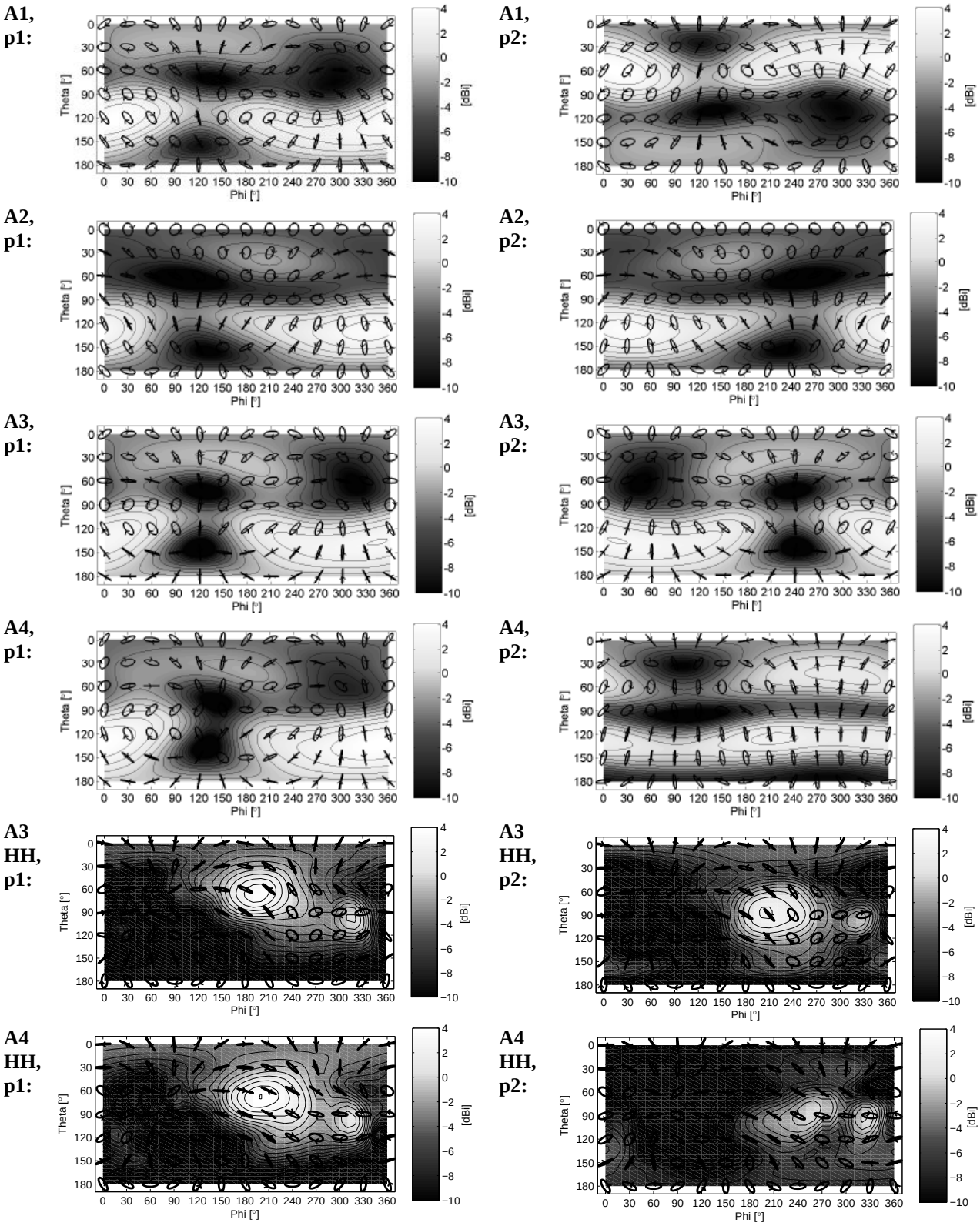

Fig. 3. Simulated 3-D realized gain patterns and polarization ellipses for A1, A2, A3, A4, A3HH, and A4HH (p1 = patch 1 & p2 = patch 2)[1]. Marking "HH" denotes that the user's head and hand have been included in the simulations.

[1] *The visualization software [36] by courtesy of Jussi Rahola (NRC/Finland)*

TABLE II, PARAMETERS OF THE SIMO AND MIMO ENVIRONMENTS USED IN THE STUDY.

SIMO environments	**Route type**	**Route length [m]****	**#Samples****	**Tx ant. type**	**Tx ant. height [m]**	**Tx ant. polarization**
Indoor Picocell	PLOS	60	1717	zig-zag array	3.2	VP
Microcell 1	NLOS	170	6030	GSM1800 BS ant.	8	VP
Microcell 2	PLOS	270	9633	GSM1800 BS ant.	8	VP
Microcell 3	NLOS	220	7933	GSM1800 BS ant.	8	VP
Macrocell 1	NLOS	230	8388	GSM1800 BS ant.	≈ 17*	VP
Macrocell 2	NLOS	300	10774	GSM1800 BS ant.	≈ 17*	VP
Macrocell 3	NLOS	440	15678	GSM1800 BS ant.	≈ 17*	VP
Highway Macrocell	PLOS	1730	12361	GSM1800 BS ant.	≈ 17*	VP
MIMO environments	**Route type**	**Route length [m]**	**#Samples****	**Tx ant. type**	**Tx ant. height [m]**	**Tx ant. polarization**
Indoor Picocell	PLOS	60	1717	zig-zag array	3.2	2*VP+2*HP
Microcell 1	LOS	90	2500	zig-zag array	13	2*VP+2*HP
Microcell 2	PLOS	180	5189	zig-zag array	13	2*VP+2*HP
Macrocell 1	NLOS	50	1342	zig-zag array	17*	2*VP+2*HP

* Transmit antennas were located at or above the rooftop level of buildings.

** Each antenna configuration was driven through each environment in five different azimuth orientations (see section V-A for more details). Therefore, actually five times longer routes and larger number of samples than given in the table were studied in this paper.

IV. EVALUATED ENVIRONMENTS

For SIMO analysis, in total eight previously measured (see [15]) routes were selected from the channel library of the Radio Laboratory of the Helsinki University of Technology (TKK). For MIMO analysis, in total four routes were selected. The selected environments include line-of-sight (LOS), non-line-of-sight (NLOS), and partly-line-of-sight (PLOS) routes. The PLOS routes are a combination of LOS and NLOS routes. The routes were grouped into four distinctive environment classes: Indoor Picocell, Microcell, Macrocell and Highway Macrocell. The Indoor Picocell route has been measured inside the Computer Science and Engineering building of TKK. The Microcell and Macrocell routes have been measured in the center of Helsinki. In the Highway Macrocell route, the spherical array has been located in the front seat of a person car moving (speed circa 14 m/s) along a highway during high traffic. Two kinds of transmit (Tx) antennas have been used in the channel measurements; a linear zig-zag array with 8 directive dual-polarized (vertical (VP) and horizontal (HP) polarizations) patch elements, and a modified vertically polarized GSM1800 base station antenna. In the MIMO performance analysis, the vertically and horizontally polarized feeds from the left- and rightmost elements (relative distance 3.5 λ) of the zig-zag array were used as transmit antennas. Table II summarizes some of the most important parameters of the selected environments.

V. COMPUTATION AND ANALYSIS METHODS

A. Antenna Rotations

As well known, the azimuth orientation of a mobile terminal can be considered random under realistic usage conditions. The random azimuth orientation was modeled by rotating the radiation patterns of each AUT in 72 degree steps to five different azimuth orientations. In Fig. 2, this corresponds to rotating the AUTs around the z-axis. In Fig. 3, this corresponds to moving the patterns in parallel with the phi-axis. Channel matrices, $\mathbf{H}^{(i)}$ ($i = 1 \ldots N_S$, where N_S is the number of samples), were after the rotations computed separately for each terminal orientation using MEBAT. At the end, the obtained five channel matrices were concatenated, as if they would represent just a single long route. As an obvious extra advantage of using the above-described method, the amount of simulation data is increased substantially, improving the statistical reliability of the analysis.

B. Normalization

The total power received by an ideal isotropic antenna is readily available from MEBAT, and was used in this work for two purposes: in the removal of large scale fading from the channel matrices (normalization), and as a reference in the computation of Effective Array Gain. Normalization of the channel matrices obtained in a given environment with the AUTs was carried out with the sliding average (length 101 samples) of the instantaneous total power received by the isotropic antenna in the same environment. For computation of Effective Array Gain, large scale fading was similarly removed from the channel matrices obtained with the isotropic antenna.

C. Envelope Correlation

In the SIMO analysis, envelope correlations for the antenna configurations were computed in a standard manner from the normalized channel matrices using [3]

$$\rho = \frac{\sum_{i=1}^{N_S}\left[r_1^{(i)} - \bar{r}_1\right]\left[r_2^{(i)} - \bar{r}_2\right]}{\sqrt{\sum_{i=1}^{N_S}\left[r_1^{(i)} - \bar{r}_1\right]^2}\sqrt{\sum_{i=1}^{N_S}\left[r_2^{(i)} - \bar{r}_2\right]^2}}, \quad (1)$$

where N_S is the number of samples and $r_{1,2}^{(i)}$ are the normalized signal envelopes with averages $\bar{r}_{1,2}$, where subscript indices 1 and 2 refer to the diversity branches. In the MIMO analysis, first envelope correlations between all possible combinations of two elements of the normalized 4x2 channel matrix were computed using (1). Correlation for the MIMO system was after this calculated as the average over the non-diagonal elements of the correlation matrix, like in [24].

D. Effective Array Gain (EAG)

Effective Array Gain is defined as the ratio of the total power received by an antenna configuration at a given cumulative probability of occurrence (p) to the total power received by an isotropic antenna at the same probability of occurrence, both obtained in the same physical channel [25]. The procedure of computing *EAG* is illustrated in Fig. 4. In this work, the *EAG*s obtained at two cumulative probability levels, p = 1% and p = 50%, were used in the SIMO and MIMO performance analysis of the studied antenna configurations. The combining method used throughout the work was Maximum Ratio Combining (MRC).

At 50% cumulative probability, *EAG* is closely related to *MEG*, and describes the power reception ability of an antenna configuration at median level. At 1% cumulative probability, *EAG* can be used to describe the low-SNR power reception ability of an antenna configuration. A theoretical estimate for *EAG* at 50 % cumulative probability can be obtained by modifying the theoretical formula of *MEG* [17] to account for multi-antenna reception:

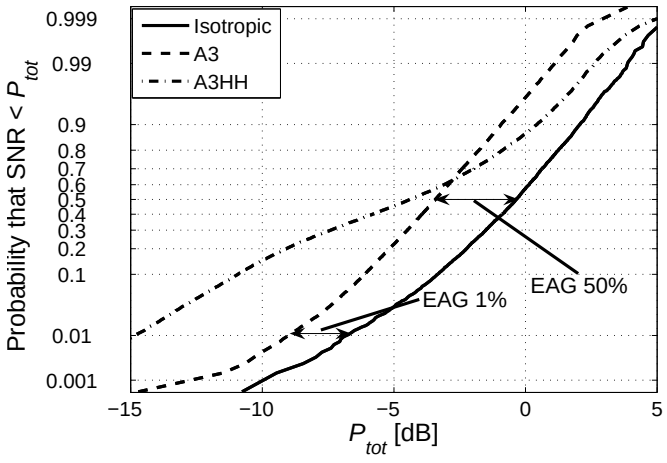

Fig. 4. Lognormal cumulative probability plots for the total powers (P_{tot}) received by A3, A3HH and the isotropic reference antenna in MIMO environment Microcell 2. The procedure of computing *EAG* at p = 1% and p = 50% cumulative probability levels is illustrated with double arrows.

$$EAG_{theo,\theta} = \int\left\{\frac{XPR}{1+XPR}\left(G_{1,\theta}(\Omega)+G_{2,\theta}(\Omega)\right)\cdot p_\theta(\Omega)\right\}d\Omega \quad (2)$$

$$EAG_{theo,\phi} = \int\left\{\frac{1}{1+XPR}\left(G_{1,\phi}(\Omega)+G_{2,\phi}(\Omega)\right)\cdot p_\phi(\Omega)\right\}d\Omega \quad (3)$$

$$EAG_{theo} = EAG_{theo,\theta} + EAG_{theo,\phi}, \quad (4)$$

where $G_{1,\theta}$ / $G_{2,\theta}$ and $G_{1,\phi}$ / $G_{2,\phi}$ are the θ and ϕ-polarized components of the realized gain patterns of diversity branches 1 and 2, *XPR* is cross polarization ratio (the ratio of the mean powers of incident theta- and phi-polarized plane waves [17]), Ω is space angle, and p_θ and p_ϕ are the angular power distribution functions of incident θ- and ϕ-polarized plane waves, respectively. For analysis purposes, the equation of EAG_{theo} has been divided into two parts representing the effective gains of an antenna configuration in theta- ($EAG_{theo,\theta}$) and phi- ($EAG_{theo,\phi}$) polarizations. Angular power distribution in azimuth was assumed uniform throughout the work. Three different elevation power distributions were studied: a uniform distribution, a double-exponential distribution [15], and a simple rectangular distribution defined as:

$$\begin{aligned} p_\theta(\theta,\phi) = p_\phi(\theta,\phi) &= P, \qquad \theta_1 \le \theta \le \theta_2 \\ &= 0 \qquad \text{otherwise,} \end{aligned} \quad (5)$$

where P is set so that

$$\int_0^{2\pi}\int_0^{\pi} p_\theta(\theta,\phi)\sin\theta\,\mathrm{d}\theta\mathrm{d}\phi = \int_0^{2\pi}\int_0^{\pi} p_\phi(\theta,\phi)\sin\theta\,\mathrm{d}\theta\mathrm{d}\phi = 1 \quad (6)$$

The uniform distribution is simply defined such that $p_\theta = p_\phi = 1/4\pi$ at all angles, which satisfies (6). For the double-exponential distribution, the average parameter values reported in [15] were used. Elevation angles θ_1 and θ_2 for the rectangular distribution were determined from the double-exponential distribution. From the *cdf* of the double-exponential distribution, it is found that at the probability of 99%, an incident plane wave is arriving between elevation angles θ_1 = 50° and θ_2 = 108°. These values were used in (5). Based on the measured results reported in [15], the average XPR in a typical urban environment with a vertically polarized transmit antenna is roughly 9 dB. This value was thus used in (2) and (3) in the theoretical SIMO study of this paper. As an exception to the above, an *XPR* of 0 dB was always used with the uniform distribution. When both vertically and horizontally polarized transmit antennas are used, it can be expected that the vertically and horizontally polarized components are roughly equal at the receiver. An XPR of 0 dB was thus used in the theoretical MIMO study of this paper.

E. Capacity and Eigenvalue Dispersion

The theoretical maximum capacity of a MIMO system in which the channel is not known by the transmitter can be found from [18],[19]

$$C = \log_2 \left| \mathbf{I} + (\rho / n_t)\mathbf{H}_N \mathbf{H}_N^H \right| \quad \text{[bit/s/Hz]}, \qquad (7)$$

where $(\,)^H$ is complex conjugate transpose, $\mathbf{I}$ is identity matrix, n_t is the number of transmit antennas, ρ is average SNR at the receiver, and $\mathbf{H}_N$ is normalized channel matrix. In this work, the capacities obtained with the SNR of 10 dB were studied at two cumulative probability levels; p = 1% and p = 50%. Also, short conclusions will be given on the effect of sweeping SNR from -10 dB to 30 dB on capacity results. One should note that the term $\mathbf{W} = \mathbf{H}_N \mathbf{H}_N^H$ in (7) can be divided into several terms, one of which represents the mean effective gain of an antenna configuration [37]. This way, the SNR in (7) becomes directly affected by the radiation properties of the antenna configuration.

In addition to the SNR, the capacity of a MIMO system is affected by the distribution of the eigenvalues of **W** [19],[38]. In theory [39], increasing the correlation between the elements of **H** increases the relative spread between the eigenvalues of **W**. The optimum situation at high-SNR is obtained when the eigenvalues of **W** are equal [38]. The spread between the eigenvalues can be characterized e.g. by the so-called eigenvalue dispersion (here denoted by *EVD*), as described in [31]. Eigenvalue dispersion gets values between $0 \leq EVD \leq 1$, where the maximum value (optimum) represents the case of equal eigenvalues, i.e. parallel information channels. In this work, eigenvalue dispersions were studied at two cumulative probability levels; p = 1% and p = 50%.

VI. Results

A. SIMO Environments

1) Envelope Correlation: Table III presents the average envelope correlation coefficients (ρ_{ave}) obtained with the studied antenna configurations in the SIMO environments. The presented values are averages over the envelope correlations obtained in the eight SIMO environments with a given antenna configuration. Comparison of the results with Table I reveals no logical connection between isolations and average envelope correlations. As a general observation, the envelope correlations are reasonably low ($\rho_{ave} \leq 0.54$), indicating a good diversity potential for all antenna configurations [1]. As an additional note, the envelope correlations seem to fall very close to each other.

2) Effective Array Gain (EAG): Average experimental Effective Array Gains ($EAG_{ave,exp}$) obtained at 1% and 50% cumulative probabilities are given in Table III. Table III also presents theoretical *EAG*s obtained with the uniform ($EAG_{uni,theo}$), double-exponential ($EAG_{dex,theo}$), and rectangular ($EAG_{rect,theo}$) angular density functions. Complete empirical results are presented in Fig. 5.

According to Table III, the theoretical *EAG*s obtained with the double-exponential and rectangular distributions fall very close to the average experimental *EAG*s obtained at the 50% cumulative probability level. The uniform distribution, instead, clearly fails in predicting the experimental results. One should note that the theoretical *EAG* obtained with the uniform distribution in fact represents the average total efficiency of an AUT (see Table I for total efficiencies). By further comparing the $EAG_{ave,exp}$ results in Table III, the following relative ranking for the antenna configurations can be obtained at both 1% and 50% cumulative probabilities: 1. A1, 2. A4, 3. A2, 4. A3, 5. A3HH, 6. A4HH. According to Table III, the same ranking is obtained theoretically with the rectangular distribution. The uniform and double-exponential distributions, on the contrary, fail to put the antenna configurations perfectly in the right order.

The relative ranking between the antenna configurations can be explained by examining the polarizations, directivities and directions of the main lobes of the radiation patterns. At both 1% and 50% cumulative probabilities, the Effective Array Gains of A1 and A4 are clearly higher than those of A2 and A3. Both A1 and A4 have main lobes pointing above the azimuth plane ($0° \leq$ theta $\leq 90°$), in which region most of the incident signal power is concentrated [15]. The main lobes of A2 and A3, on the contrary, are pointing towards the ground, which explains the difference. At 50% cumulative probability, the Effective Array Gains of A3 and A4 are clearly lower in talk position than in free space, which is mainly explained by the low total efficiencies of A3HH and A4HH. At 1% cumulative probability, the difference between the talk position and free space results is even larger. A logical explanation for this can be found by examining the widths of the main lobes. In free space, the main lobes of A3 and A4 quite uniformly cover the whole azimuth angle range ($0° \leq$ phi $\leq 360°$), whereas in the talk position, they are much narrower. With a very narrow pattern, the probability of receiving only weak signal becomes high [24], degrading *EAG* at the lower cumulative probabilities.

TABLE III, Average Envelope Correlations (ρ_{ave}), Average Experimental Effective Array Gains ($EAG_{AVE,EXP}$), and Theoretical Effective Array Gains ($EAG_{UNI,THEO}$, $EAG_{DEX,THEO}$ and $EAG_{RECT,THEO}$) Obtained in the SIMO Environments.

	A1	**A2**	**A3**	**A4**	**A3HH**	**A4HH**
ρ_{ave}	0.38	0.40	0.29	0.25	0.48	0.54
$EAG_{ave,exp}$ **1% [dBi]**	4.6	2.9	2.5	4.2	0.1	-0.7
$EAG_{ave,exp}$ **50% [dBi]**	-1.3	-3.5	-4.0	-2.4	-4.5	-5.1
$EAG_{uni,theo}$ **[dBi]**	-1.0	-2.0	-1.4	1.2	-4.7	-5.0
$EAG_{dex,theo}$ **[dBi]**	-1.8	-3.6	-4.4	-3.1	-4.2	-4.8
$EAG_{rect,theo}$ **[dBi]**	-1.0	-3.3	-3.9	-1.8	-4.4	-5.4

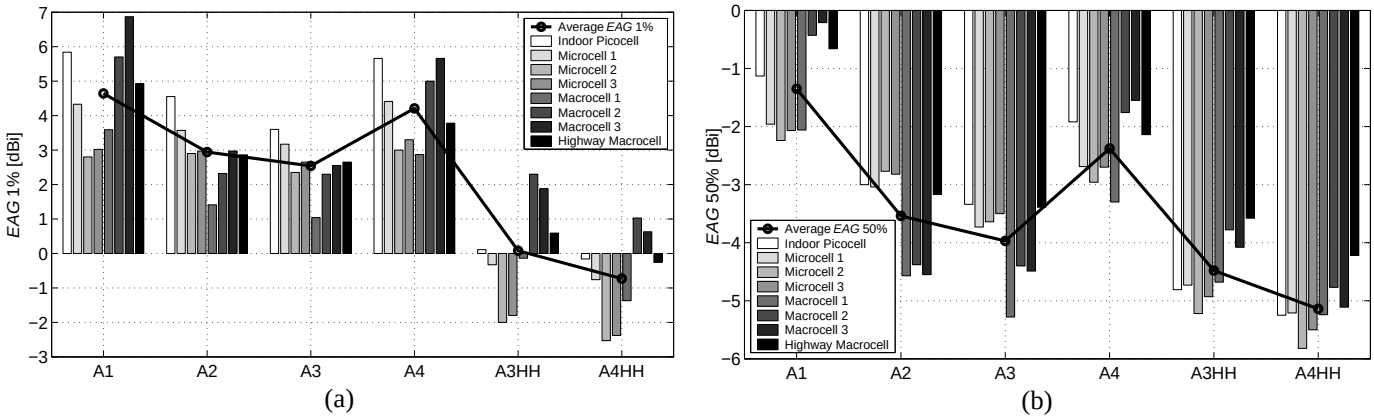

Fig. 5. Experimental Effective Array Gains (*EAG*) obtained in the SIMO environments at (a) 1% (b) 50% cumulative probability levels. The circles represent averages over the studied environments.

As an interesting observation from Fig. 5, it can be seen that the *EAG*s are mainly positive at the 1% cumulative probability level. At the 50% cumulative probability, instead, the *EAG*s are negative. At 1% cumulative probability, A1-A4 thus perform better than the isotropic reference antenna. This is expected, as the studied antenna configurations have the advantage of diversity combining compared to the single reference antenna. Also, polarizations of the main lobes of A1-A4 fairly well match with the vertical polarization of the incident signal power. At the 50% cumulative probability, the uniform pattern (0 dBi gain) of the isotropic reference antenna works very well by outperforming the patterns of A1-A4.

B. MIMO Environments

1) Envelope Correlation: Table IV presents the average envelope correlation coefficients (ρ_{ave}) obtained with the studied antenna configurations in the MIMO environments. As a general observation, the antenna configurations again have nearly equal average envelope correlation coefficients.

2) Effective Array Gain (EAG): Experimental average Effective Array Gains ($EAG_{ave,exp}$) obtained at the 1% and 50% cumulative probabilities are presented in Table IV and complete results in Figs. 6 (a)-(b). Table IV also presents the theoretical Effective Array Gains obtained with the uniform ($EAG_{uni,theo}$), double-exponential ($EAG_{dex,theo}$), and rectangular ($EAG_{rect,theo}$) power density functions. Furthermore, the theta- ($EAG_{rect,theo,\theta}$) and phi- ($EAG_{rect,theo,\phi}$) components of $EAG_{rect,theo}$ are reported.

With the double-exponential and rectangular distributions, the theoretically predicted *EAG*s again fall very close to the median $EAG_{ave,exp}$, whereas the uniform distribution clearly fails in predicting the experimental results. By further comparing the median $EAG_{ave,exp}$ results in Table IV, the following relative ranking for the studied antenna configurations can be obtained: 1. A1, 2. A4, 3. A3, 4. A3HH, 5. A2, 6. A4HH. According to Table IV, the same ranking is obtained theoretically with the rectangular angular power distribution. The uniform and double-exponential distributions again fail in putting the antenna configurations in the right order. The proposed rectangular distribution thus seems to offer a quick and reliable way of estimating and comparing the average *EAG*s obtained with realistic antenna configurations under realistic channel conditions.

TABLE IV, AVERAGE ENVELOPE CORRELATION COEFFICIENTS (ρ_{ave}), AVERAGE EXPERIMENTAL EFFECTIVE ARRAY GAINS ($EAG_{AVE,EXP}$), THEORETICAL EFFECTIVE ARRAY GAINS ($EAG_{UNI,THEO}$, $EAG_{DEX,THEO}$, $EAG_{RECT,THEO}$, $EAG_{RECT,THEO,\theta}$ AND $EAG_{RECT,THEO,\phi}$), AVERAGE EIGENVALUE DISPERSIONS (EVD_{AVE}), AND AVERAGE CAPACITIES (C_{AVE}) OBTAINED IN THE MIMO ENVIRONMENTS.

	A1	**A2**	**A3**	**A4**	**A3HH**	**A4HH**
ρ_{ave}	0.42	0.43	0.41	0.42	0.59	0.54
$EAG_{ave,exp}$ **1% [dBi]**	-1.6	-3.1	-2.7	-2.5	-7.1	-7.7
$EAG_{ave,exp}$ **50% [dBi]**	-1.1	-3.4	-3.1	-2.8	-3.2	-3.5
$EAG_{uni,theo}$ **[dBi]**	-1.0	-2.0	-1.4	-1.2	-4.7	-5.0
$EAG_{dex,theo}$ **[dBi]**	-1.9	-3.7	-3.4	-3.6	-3.1	-3.3
$EAG_{rect,theo}$ **[dBi]**	-1.4	-3.6	-3.1	-2.7	-3.4	-3.8
$EAG_{rect,theo,\theta}$ / $EAG_{rect,theo,\phi}$ **[dBi]**	-3.9/-5.0	-6.2/-7.0	-7.1/-5.3	-4.6/-7.3	-7.7/-5.3	-9.0/-5.3
EVD_{ave} **1%**	0.3	0.3	0.2	0.3	0.3	0.2
EVD_{ave} **50%**	0.8	0.8	0.8	0.7	0.8	0.6
C_{ave} **1% [bit/s/Hz]**	1.4	1.1	1.2	1.2	0.5	0.5
C_{ave} **50% [bit/s/Hz]**	4.2	3.1	3.2	3.3	3.4	3.1

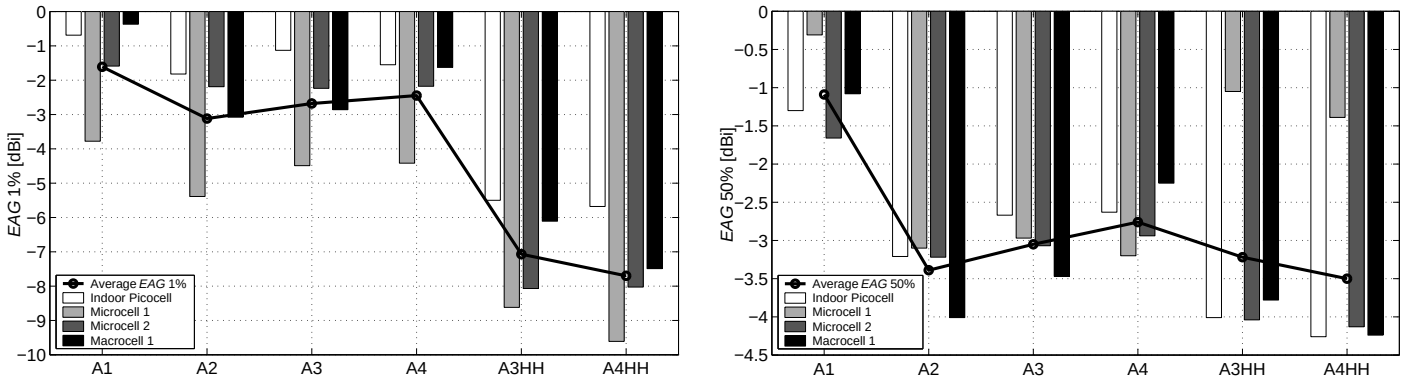

Fig. 6. Experimental Effective Array Gains (*EAG*) obtained in the MIMO environments at (a) 1% (b) 50% cumulative probability levels. The circles represent averages over the studied environments.

Despite of the low total efficiencies of A3HH and A4HH (see Table I), interestingly, their $EAG_{ave,exp}$ results at the 50% cumulative probability are at the same range with the free space results of A1 – A4. As can be seen from Table IV, A3HH and A4HH both have very high $EAG_{rect,theo,\phi}$. In other words, A3HH and A4HH radiate strongly with phi-polarization in the directions from which incident signal power is most likely arriving. When both vertically and horizontally polarized transmit antennas are used, the *EAG*s of A3HH and A4HH at the 50% cumulative probability therefore become surprisingly high. At the 1% cumulative probability, however, the $EAG_{ave,exp}$ of A3HH and A4HH again are clearly lower than those of A1 – A4. Fig. 4. illustrates the phenomenon with A3 and A3HH in MIMO environment Microcell 2. In this particular environment, A3HH with its narrow but effectively radiating (see $EAG_{rect,theo}$) pattern outperforms at high outage levels (>0.6) the more omnidirectional pattern of A3. With the narrow main lobe of A3HH, however, the probability of receiving only weak signal becomes high, which is clearly seen at the 1% cumulative probability level in Fig. 4.

From Fig. 6, it can be seen that *EAG*s are now negative at both 1% and 50% cumulative probability levels. In the SIMO environments, the polarizations (vertical) of the main lobes of A1-A4 fairly well matched with the vertical polarization of incident signal power. Partly for this reason, *EAG*s were mainly positive. In the MIMO environments, the power of incident waves is distributed roughly equally between the vertical and horizontal polarizations. For this reason most likely, A1-A4 do not perform in the MIMO environments at 1% cumulative probability as well against the isotropic reference antenna, which utilizes both polarizations. In general, isotropic radiation thus seems to be a good choice when *XPR* is close to 0 dB.

3) Eigenvalue Dispersion: Average eigenvalue dispersions (EVD_{ave}) obtained at the 1% and 50% cumulative probabilities are presented in Table IV. According to Table IV, all antenna configurations have nearly equal EVD_{ave} at both cumulative probabilities. In other words, the distributions of the eigenvalues obtained with the studied antenna configurations are in average very similar. A possible explanation for this can be found from the nearly equal average correlation coefficients. As an interesting observation, the proximity of the user's head and hand does not seem to affect the eigenvalue dispersion of a MIMO system. As a consequence of the nearly equal EVD_{ave} results, one might suspect that possible differences in the capacity results would be mainly originated from the differences in the power transferring properties of the studied antenna configurations.

4) Capacity: Complete experimental capacity results obtained at the 1% and 50% cumulative probabilities with the SNR of 10 dB are presented in Figs. 7 (a)-(b). Average capacities (C_{ave}) are also presented in Table IV. The highest capacities in the studied environments are obtained in Microcell 1 at 50% cumulative probability. This is expected, as Microcell 1 is a line-of-sight route (see Table II). At 1% cumulative probability, A1 distinguishes from the other antenna configurations with its higher average capacity, whereas A3HH and A4HH perform clearly the worst. At 50% cumulative probability, A1 again performs clearly the best, whereas the average capacities of the other AUTs fall very close to each other. As an interesting note, the above-described performance differences are clearly noticeable also in the corresponding $EAG_{ave,exp}$ results. In general, high *EAG* seems to predict high capacity, and vice versa. During the work, also the effect of SNR (ρ in (7)) on the capacity results was shortly tested by varying SNR from -10 dB to 30 dB. The results (not presented here) indicated no change in the relative ranking between the antenna configurations when the SNR was changed.

VII. Discussion and Conclusions

In this paper, four realistic multi-antenna terminals have been comprehensively studied in a large amount of measured SIMO and MIMO environments. Several performance metrics, such as the total efficiencies of the antenna configurations, envelope correlation, Effective Array Gain (*EAG*), eigenvalue dispersion, and capacity have been used in the performance evaluation. Emphasis has been put on increasing understanding on the power transferring properties of mobile terminal multi-

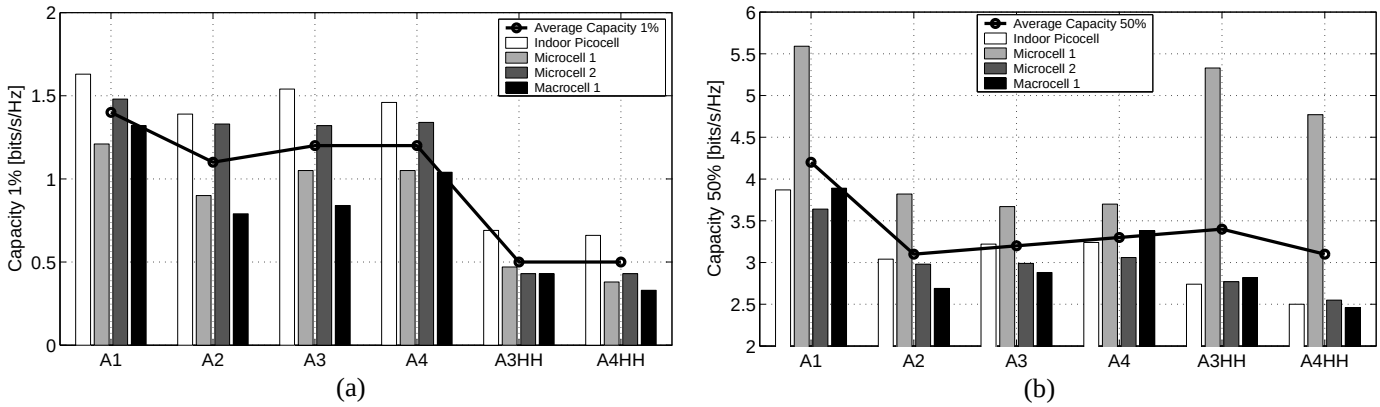

Fig. 7. Capacities obtained in the MIMO environments at (a) 1% (b) 50% cumulative probability levels. The circles represent averages over the studied environments.

antenna configurations. For this purpose, the *EAG* has been used. Also efficient theoretical ways of predicting the empirical *EAG* results based on the simulated 3-D radiation patterns of an AUT have been proposed and studied. Several interesting observations can be made from the results:

- The average envelope correlation coefficients obtained with the antenna configurations were both in the SIMO and MIMO systems fairly close to each other, and reasonably low. The contribution of envelope correlation on the *EAG* results was thus not clearly noticeable. Further lowering of the envelope correlations, however, might improve the *EAG*s of the studied antenna configurations at low cumulative probability levels. With the studied antenna configurations, no logical connection was found between the envelope correlation of an antenna configuration and the isolation (i.e. mutual coupling) between the diversity elements of the antenna configuration.
- The average (over several environments) 50% cumulative probability Effective Array Gain of an antenna configuration can be accurately estimated from the simulated 3-D radiation patterns of the antenna configuration by assuming a simple rectangular elevation power distribution for incident signals. In this study, the *EAG* estimates obtained theoretically with the rectangular distribution also ranked the antenna configurations perfectly in the same order as the experimental average *EAG*s obtained with MEBAT. Uniform and double-exponential elevation power distributions failed in correctly predicting the relative ranking between the studied antenna configurations.
- The optimum performance in terms of the *EAG* is obtained when the main lobes of an antenna configuration are oriented and polarized according to the arriving directions and polarization of incident signal power, as could be expected. Moreover, the total efficiency of an antenna configuration should be maximized. In addition to the above, the experimental *EAG*s obtained at the 1% cumulative probability were strongly affected by the widths of the main lobes of the studied antenna configurations. With a very narrow main lobe, the probability of receiving only weak signal becomes high, degrading *EAG* at lower cumulative probabilities. At the 50% cumulative probability, however, an AUT with a narrow pattern can obviously perform very well if its main lobes are well oriented and polarized with respect to the angular power spectrum of incident signals.
- In the MIMO environments, the average eigenvalue dispersions obtained with the studied antenna configurations were nearly equal. Differences in the average capacities were mainly caused by the differences in the average *EAG*s of the antenna configurations. Thus, a mobile terminal antenna designer seems to have only little control over the spatial multiplexing properties of a MIMO system when realistic multi-antenna configurations and realistic environments are considered. An antenna designer should therefore mainly focus on maximizing the power transferring properties, i.e. the Effective Array Gain, of a multi-antenna configuration.

One should finally note that optimum radiation pattern characteristics are difficult to realize in a real mobile terminal. This is because of the strong contribution of the metallic chassis of a mobile terminal on the radiation properties of the device. Moreover, user's head, hand, and other body parts significantly absorb radiation in certain directions. Optimum antenna characteristics, however, are worth pursuing and provide a direction in which to aim.

REFERENCES

[1] W. C. Jakes, Y. S. Yeh, M. J. Gans, and D. O. Reudink, *Microwave Mobile Communications*, New York, 1974, IEEE Press, 642 p.

[2] R. G. Vaughan and J. Bach Andersen, "Antenna diversity in mobile communications", *IEEE Transactions on Vehicular Technology*, Vol. VT-36, No. 4, November 1987, pp. 149-172.

[3] C. B. Dietrich, K. Dietze, J. R. Nealy, and W. L. Stutzman, "Spatial, polarization, and pattern diversity for wireless handheld terminals", *IEEE Transactions on Antennas and Propagation*, Vol. 49, No. 9, September 2001, pp. 1271 - 1281.

[4] G. F. Pedersen, S. Widell, and T. Ostervall, "Handheld antenna diversity evaluation in a DCS 1800 small cell", *The 8th IEEE International Symposium on Personal, Indoor and Mobile Radio Communications (PIMRC)*, Vol. 2, September 1997, pp. 584 – 588.

[5] B. M. Green, and M. A. Jensen, "Diversity performance of dual-antenna handsets near operator tissue", *IEEE Transactions on Antennas and Propagation*, Vol. 48, No. 7, July 2000, pp. 1017 - 1024.

[6] S. B. Yeap, X. Chen, J. A. Dupuy, C.C. Chiau, and C. G. Parini, "Low profile diversity antenna for MIMO applications", *Electronics Letters*, Vol. 42, No. 2, January 2006, pp. 69 – 71.

[7] C. C. Chiau, X. Chen, and C. G. Parini, "A compact four-element diversity-antenna array for PDA terminals in a MIMO system", *Microwave and Optical Technology Letters*, Vol. 44, No. 5, March 2005, pp. 408 – 412.

[8] Z. Ying, T. Bolin, V. Plicanic, A. Derneryd, and G. Kristensson, "Diversity antenna terminal evaluation", *Proc. IEEE Antennas and Propagation Society International Symposium*, Washington, USA, Vol. 2A, July 2005, pp. 375 – 378.

[9] Y. Zhinong, V. Plicanic, T. Bolin, G. Kristensson, and A. Derneryd, "Characterization of multi-channel antenna performance for mobile terminal by using near field and far field parameters", Proc. of the COST 273 TD(04)(095) meeting, Göteborg, Sweden, June 2004.

[10] G. A. Mavridis, E. D. Karapistoli, C. G. Christodoulou, and M. T. Chryssomallis, "Spatial diversity performance of printed dual band antennas for WLAN operations", Proc. IEEE Antennas and Propagation Society International Symposium, Washington, USA, Vol. 1A, July 2005, pp. 491 – 494.

[11] M. Karaboikis, C. Soras, G. Tsachtsiris, and V. Makios, "Compact dual-printed inverted-F antenna diversity systems for portable wireless devices", IEEE Antennas and Wireless Propagation Letters, Vol. 3, No. 1, 2004, pp. 9 – 14.

[12] P.- S. Kildal, K. Rosengren, J. Byun, and J. Lee, "Definition of effective diversity gain and how to measure it in a reverberation chamber", Microwave and Optical Technology Letters, Vol. 34, No. 1, July 2002, pp. 56 – 59.

[13] P.- S. Kildal, and K. Rosengren, "Electromagnetic analysis of effective and apparent diversity gain of two parallel dipoles", IEEE Antennas and Wireless Propagation Letters, Vol. 2, No. 1, 2003, pp. 9 – 13.

[14] J. Villanen, P. Suvikunnas, C. Icheln, J. Ollikainen, and P. Vainikainen, "Advances in diversity performance analysis of mobile terminal antennas", *International Symposium on Antennas and Propagation (ISAP'04)*, Sendai, Japan, August 2004, CD-ROM (ISBN 4-88552-208-0), paper 3A3-3.pdf.

[15] K. Kalliola, K. Sulonen, H. Laitinen, O. Kivekäs, J. Krogerus, and P. Vainikainen, "Angular power distribution and mean effective gain of mobile antenna in different propagation environments", *IEEE Transactions on Vehicular Technology*, Vol. 51, No. 5 , September 2002, pp. 823 -838.

[16] J. B. Andersen, and F. Hansen, "Antennas for VHF/UHF personal radio: A theoretical and experimental study of characteristics and performance", *IEEE Transactions on Vehicular Technology*, Vol. VT-26, No. 4, November 1977, pp. 349 - 357.

[17] T. Taga, "Analysis for mean effective gain of mobile antennas in land mobile radio environments," *IEEE Transactions on Vehicular Technology*, Vol. 39, No. 2, May 1990, pp. 117-131.

[18] I. E. Telatar, "Capacity of multi-antenna Gaussian channels", *AT&T Bell Labs Technical memorandum*, October 1995, 28 p.

[19] G. J. Foschini, M. J. Gans, "On the limits of wireless communications in a fading environment when using multiple antennas", *Wireless Personal Communications*, Vol. 6, No. 3, March 1998, pp. 311–335.

[20] G. J. Foschini, G. D. Golden, R. A. Valenzuela, and P. W. Wolniansky, "Simplified processing for wireless communication at high spectral efficiency", *IEEE Journal on Selected Areas in Communications – Wireless Communications Series*, Vol. 17, November 1999, pp. 1841 – 1852.

[21] B. Lindmark, L. Garcia-Garcia, N. Jalden, and C. Orlenius, "Evaluation of MIMO arrays using antenna patterns, reverberation chamber, and channel measurements", *European Conference on Antennas and Propagation (EuCAP'06)*, Nice, France, November 2006, CD-ROM, paper 372151bl.pdf.

[22] D. W. Browne, M. Manteghi, M. P. Fitz, and Y. Rahmat-Samii, "Experiments with compact antenna arrays for MIMO radio communications", *IEEE Transactions on Antennas and Propagation*, Vol. 54, No. 11, November 2006, pp. 3239 – 3250.

[23] C. Waldschmidt, C. Kuhnert, S. Schulteis, and W. Wiesbeck, "On the integration of MIMO systems into handheld devices", *Proc. ITG Workshop on Smart Antennas*, München, Germany, March 2004, pp. 1 - 8.

[24] J. Salo, B. Badic, P. Suvikunnas, H. Weinrichter, M. Rupp, and P. Vainikainen, "Performance of space-time block codes in urban microcells: the effect of antennas", *International Symposium on Wireless Personal Multimedia Communications (WPMC'05)*, Aalborg, Denmark, September 2005, pp. 1848 - 1852.

[25] C. Waldschmidt, S. Schulteis, and W. Wiesbeck, "Complete RF system model for analysis of compact MIMO arrays", *IEEE Transactions on Vehicular Technology*, Vol. 53, No. 3, May 2004, pp. 579 – 586.

[26] V. Jungnickel, V. Pohl, and C. V. Helmolt, "Capacity of MIMO systems with closely spaced antennas", *IEEE Communications Letters*, Vol. 7, No. 8, August 2003, pp. 361-363.

[27] P. Kyritsi, D. C. Fox, R. A. Valenzuela, and P. W. Wolniansky, "Effect of antenna polarization on the capacity of multiple element system in an indoor environment", *IEEE Journal on Selected Areas in Communications*, Vol. 20, No. 6, August 2002, pp. 1227-1239.

[28] D. Chizhik, J. Ling, P. W. Wolniansky, R. A. Valenzuela, N. Costa, and K. Huber, "Multiple-Input-Multiple-Output Measurements And Modeling in Manhattan", *IEEE Journal on Selected Areas in Communications*, Vol. 21, No. 3, April 2003, pp. 321-331.

[29] P. Vainikainen, J. Ollikainen, O. Kivekäs, and I. Kelander, "Resonator-based analysis of the combination of mobile handset antenna and chassis", *IEEE Transactions on Antennas and Propagation*, Vol. 50, No. 10, October 2002, pp. 1433-1444.

[30] P. Suvikunnas, J. Villanen, K. Sulonen, C. Icheln, J. Ollikainen, and P. Vainikainen, "Evaluation of the performance of multiantenna terminals using a new approach", *IEEE Transactions on Instrumentation and Measurement*, Vol. 55, No. 5, October 2006, pp. 1804 - 1813.

[31] J. Salo, P. Suvikunnas, H. M. El-Sallabi, and P. Vainikainen, "Some insights into MIMO mutual information: the high SNR case", *IEEE Transactions on Wireless Communications*, Vol. 5, No. 11, November 2006, pp. 2997 - 3001.

[32] J. Kivinen, T. Korhonen, P. Aikio, R. Gruber, P. Vainikainen and S.-G. Häggman, "Wideband radio channel measurement system at 2 GHz", *IEEE Transactions on Instrumentation and Measurement*, Vol. 48, February 1999, pp. 39–44.

[33] K. Kalliola, H. Laitinen, L. Vaskelainen, and P. Vainikainen, "Real-time 3-D spatial-temporal dual-polarized measurement of wideband radio channel at mobile channel", *IEEE Transactions on Instrumentation and Measurement*, Vol. 49, No. 2, April 2000, pp. 439-448.

[34] J. Ollikainen, O. Kivekäs, A. Toropainen, and P. Vainikainen, "Internal dual-band patch antenna for mobile phones", *Proceedings of the AP2000 Millennium Conference on Antennas and Propagation*, Davos, Switzerland, April 2000, paper p1111.pdf.

[35] O. Kivekäs, J. Ollikainen, T. Lehtiniemi, and P. Vainikainen, "Bandwidth, *SAR*, and efficiency of internal mobile phone antennas", *IEEE Transactions on Electromagnetic Compatibility*, Vol. 46, No. 1, February 2004, pp. 71 - 86.

[36] J. Rahola and J. Krogerus, "On the polarization states of mobile terminals", *Proc. 12th International Conference on Antennas and Propagation*, Vol. 2, Exeter, UK, April 2003, pp. 695-698.

[37] P. Suvikunnas, J. Salo, J. Kivinen, and P. Vainikainen, "Empirical comparison of MIMO antenna configurations", *IEEE Vehicular Technology Conference (VTC'2005 Spring)*, Stockholm, Sweden, June 2005, Vol. 1, pp. 53 – 57.

[38] N. Chiurtu, B. Rimoldi, and E. Telatar, "On the capacity of multi-antenna gaussian channels", *Proc. IEEE International Symposium on Information Theory*, Washington, USA, June 2001, pp. 53.

[39] D.– S. Shiu, G. J. Foschini, M. J. Gans, and J. M. Kahn, "Fading correlation and its effect on the capacity of multielement antenna systems", *IEEE Transactions on Communications*, Vol. 48, No. 3, March 2000, pp. 502 – 513.

Juha Villanen was born in Helsinki, Finland, 1979. He received the degree of Master of Science in Technology from Helsinki University of Technology (TKK) in 2003. He is currently working towards the degree of Doctor of Science in Technology.

From 2002 until fall 2007, he worked as a research engineer at the Radio Laboratory of TKK. In fall 2007, he joined Nokia Mobile Phones in Oulu. His research interests include miniaturization and evaluation methods of mobile terminal antenna structures.

Pasi Suvikunnas was born in Tuusula, Finland, in 1967. He received the B. Sc. in technology from Technical Institute of Helsinki in 1994. He received the M. Sc., L. Sc. and D. Sc. degrees in technology from Helsinki University of Technology (TKK) in 1999, 2002 and 2006, respectively.

Since 1999, he has been with the Radio Laboratory of HUT as a Researcher. His current fields of interest are multielement antennas and mobile radio propagation.

Clemens Icheln was born in Hamburg, Germany, in 1968. He received the M.Sc. degree in Electrical Engineereing at Hamburg-Harburg University of Technology, Germany, in 1996, the Licentiate degree in Radio Engineering and the Doctor of Science in Technology degree at Helsinki University of Technology (TKK), Finland, in 1999 and 2001, respectively.

He has experience in the fields of design of mobile terminal antennas and their evaluation methods. He is currently working as a leading scientist at the SMARAD/Radio Laboratory of TKK.

Jani Ollikainen was born in Lahti, Finland, in 1971. He earned the Master of Science in Technology, Licentiate of Science in Technology, and Doctor of Science in Technology degrees in electrical and communications engineering in 1997, 2000, and 2004, respectively, from Helsinki University of Technology (TKK).

From 1996 until 2003, he worked as a Researcher at the Radio Laboratory of TKK. In early 2003, he joined Nokia Research Center in Helsinki, Finland, where he is currently working as a Research Manager. His research interests include design, implementation, and measurement techniques of small antennas for personal mobile communications.

(Jani Ollikainen is a member of IEEE since 2003.)

Pertti Vainikainen (M'91) received the degree of Master of Science in Technology, Licentiate of Science in Technology and Doctor of Science in Technology from Helsinki University of Technology (TKK) in 1982, 1989 and 1991, respectively.

From 1992 to 1993 he was Acting Professor of Radio Engineering, since 1993 Associate Professor of Radio Engineering and since 1998 Professor in Radio Engineering, all in the Radio Laboratory of TKK. In 1993-97 he was the director of the Institute of Radio Communications (IRC) of TKK, and a visiting professor in 2000 at Aalborg University, Denmark and in 2006 at University of Nice in France. His main fields of interest are antennas and propagation in radio communications and industrial measurement applications of radio waves. He is the author or co-author of 6 books or book chapters and over 270 refereed international journal or conference publications and the holder of 9 patents.